Applied Physics A (2018) 124:544
https://doi.org/10.1007/s00339-018-1962-1

Applied Physics A
Materials Science & Processing

Reaction kinetics of equiatomic Fe–Mo solid solutions obtained by mechanical alloying: an X-ray diffraction and Mössbauer spectroscopy study

F. I. S. Silva[1] · M. S. Pereira[2] · I. F. Vasconcelos[1]

Received: 19 April 2018 / Accepted: 7 July 2018 / Published online: 18 July 2018

Abstract
The reaction kinetics of equiatomic Fe–Mo solid solutions produced by mechanical alloying were studied by X-ray diffraction and Mössbauer spectroscopy. The materials were milled with velocities of rotation of 400 and 500 rpm for several milling times to obtain samples of various reaction stages. The X-ray diffraction patterns showed the presence of two bcc phases, corresponding to metallic Fe and Mo, in all samples. Analysis of these diffractograms indicated diffusion of Mo within the Fe matrix and diffusion of Fe within the Mo matrix, as a result of the milling process. While the X-ray diffraction technique did not allow for the identification of a crystallographic phase being clearly transformed, making it difficult to study the reaction kinetics, using Mössbauer spectroscopy, it was possible to identify two magnetic phases that suffer transformation during the course of milling: a ferromagnetic sextet corresponding to metallic Fe and a paramagnetic doublet corresponding to Fe atoms with a majority of Mo neighbors (metallic Mo does not possess a magnetic moment). Both magnetic phases may be present in the bcc Fe matrix or the bcc Mo matrix. The transformation kinetics of the sextet were studied using a method based on a local description of phase volume transformation, depicted by the tribochemical activity parameter. The results were compared to published work on the application of this method to Fe–Cu and Fe–N systems. A behavior similar to that of Fe–N was observed, which, similar to the Fe–Mo system and as opposed to the Fe–Cu system, possesses a positive enthalpy of mixing.

1 Introduction

Iron-based solid solutions including steels have been intensively studied for years because of their importance as construction materials for the modern industry and engineering. Among the systems commonly studied, solid solutions with Fe–Mo chemical composition have attracted the interest of several research groups [1–8]. Nowadays, many techniques have been employed for the synthesis of metallic alloys, such as mechanical alloying [9–13], sol–gel method [14, 15], arc furnace [5, 6, 16], electrodeposition [2], among others.

Mechanical alloying (also known as mechanosynthesis) is an inexpensive, efficient and extremely flexible (albeit complex) technique for the production of solid-state reactions between powdered materials. In a typical mechanical alloying experiment, reactant powders and milling balls are inserted in a jar and submitted to grinding in a ball mill. Several parameters can influence the final result of the process, such as the milling tools, ball-to-powder mass ratio, shock frequency, milling energy and milling time [17–20]. These parameters can still have different effects for each type of mill.

Owing to its simplicity and flexibility, mechanosynthesis has grown more and more in importance as studies of the influence of the reaction parameters on the final product are developed [4, 16, 21, 22]. Although the empirical process is well known and experimentally established, the difficulties in describing a process of such complexity are barriers to further study. A quantitative description of mechanosynthesis is very important and necessary to establish a way to predict the outcome of the process or at least to determine which actual physical parameters are responsible for the final milling product.

✉ M. S. Pereira
mauriciosousa@alu.ufc.br

[1] Department of Metallurgical and Materials Engineering, Universidade Federal do Ceará, Fortaleza, Brazil

[2] Laboratory of Telecommunications and Materials Science and Engineering, Department of Physics, Universidade Federal do Ceará, Fortaleza, Brazil

Mechanical alloying is based on the energy transfer from the milling tools to solid powder mixtures through impacts. In each impact, a small amount of powder is trapped between impacting balls or between a ball and milling container walls. The mechanosynthesis process is the result of repeated fracture and welding of the powder particles as a result of these impacts. Therefore, impact characteristics, such as energy and frequency, are determinant to the result. Planetary mills are the most commonly used type of mill and models to calculate these parameters based on characteristics of powders, milling tools, and mill itself have been proposed and successfully applied [19, 23]. Models based on thermodynamics have also been used to provide insights into the reactions occurring inside the milling jar [19, 23].

Another possible approach to study mechanical alloying mechanisms is to formulate kinetic laws based on a local description of phase transformations in the course of the process. A local description of mechanical alloying involves the morphological conditions of the materials, the way in which they respond to high compressions, the chemical affinities between them and how the milling conditions influence the overall process. This description can be achieved using measured global parameters, such as the phase volumes. Phase decomposition and formation induced by solid-state reactions are often empirically described by Johnson–Mehl–Avrami (JMA)-type equations [7, 8, 18, 24–26].

Vasconcelos and de Figueiredo [18] proposed and developed a model in an attempt to describe the local mechanism of mechanical alloying. This model is based on the observation of global parameters, such as the volumes of the various phases present in the material and their transformations during the process. A certain amount of α phase is created after a mechanical alloying-driven solid-state reaction between two other phases, β and γ. The authors assert that the volume created or transformed ΔV_α after an impact involving a $\beta\gamma$ interface between phases is a function of the probability to find a $\beta\gamma$ interface ($P_{\beta\gamma}(t)$) and tribochemical activity ($\xi^{\alpha}_{\beta\gamma}(t)$).

The tribochemical activity is a rough measure of the tendency of β and γ to react to form α, including many aspects, such as chemical activities, morphologies of components and impact characteristics (energy, frequency and so on). The analysis is greatly simplified considering a system composed of two phases, which may be crystallographic, magnetic or otherwise, where one phase is transformed in the other in the course of milling. Therefore, the tribochemical activity to create or destroy phase ϵ can be written as

$$\xi^{\epsilon}(t) \propto \frac{\mathrm{d}V_{\epsilon}(t)}{\mathrm{d}t}\frac{1}{V_{\epsilon}(t)\left[1-V_{\epsilon}(t)\right]}, \tag{1}$$

where $V_\epsilon(t)$ is the relative volume of phase ϵ in the sample at a given instant of time t.

The goal of this work is to study the reaction kinetics of a mechanically alloyed equiatomic Fe–Mo solid solutions from a tribochemical activity-based local description of volume phases time evolution using X-ray diffraction and Mössbauer spectroscopy results.

2 Experimental

Solid solutions of equiatomic Fe–Mo were prepared by mechanical alloying. Elemental iron and molybdenum powders (purity ≥ 99%), and stainless steel vial and balls (12 balls; ball-to-powder mass ratio of 20:1) were used in a Fritsch Pulverisette 6 planetary mill operating with angular velocities of 400 and 500 rpm. To produce each sample, a fresh Fe–Mo mixture was milled for the designed time in milling periods of 30 min with 10-min pauses in between to avoid overheating. The presence of dissolved oxygen seems to influence the reaction [27]; therefore, to minimize oxygen contamination the vial was closed and sealed in inert Ar atmosphere and was never opened or taken out of the mill during the entire process.

X-ray diffraction patterns were collected at room temperature using a Rigaku DMAXB diffractometer operating with a Kα-Cu source ($\lambda = 1.54$ Å) with angle 2θ ranging from 30° to 90°. Rietveld refinement procedures [28, 29] were applied to all the X-ray diffraction patterns using DBWSTools 2.3 [30] software. Reference cards from the Inorganic Crystal Structure Database were used to refine the bcc Fe (ICSD-64998) and bcc Mo (ISCD-76147) patterns.

Room temperature Mössbauer spectra were measured in transmission mode using a 57 Co(Rh) radioactive source mounted on a velocity driver operating in sinusoidal mode. The data were evaluated by least square fitting to a series of discrete Lorentzian-shaped subspectra by means of the software package Normos. Isomer shifts (δ) are quoted with respect to α-Fe.

3 Results and discussion

Figure 1 shows the X-ray diffractograms of an unmilled sample and samples ground at 400 rpm for 1, 2 and 4 h. Experimental data are shown as black circles while Rietveld refinements are shown as red lines. The diffractograms reveal the presence of Fe and Mo phases, both with a bcc structure. It is possible to observe diffraction peak broadening with the increase of milling time, which is a consequence of the average grain size reduction induced by milling. In addition, it can be observed that both the bcc Fe and bcc Mo structures are maintained throughout the course of milling.

The lattice parameter, a, of each phase and for each milling time is shown in Table 1. It is possible to observe a slight

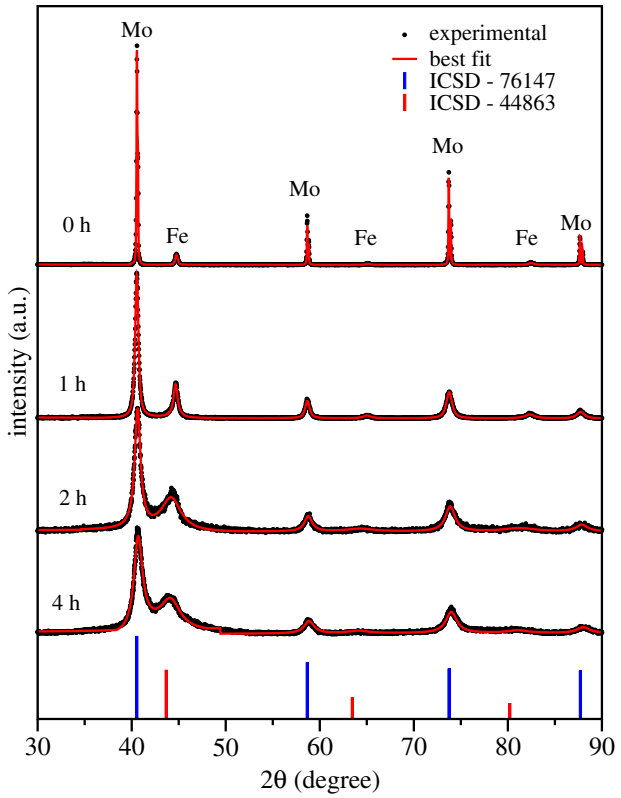

Fig. 1 X-ray patterns of samples milled at 400 rpm

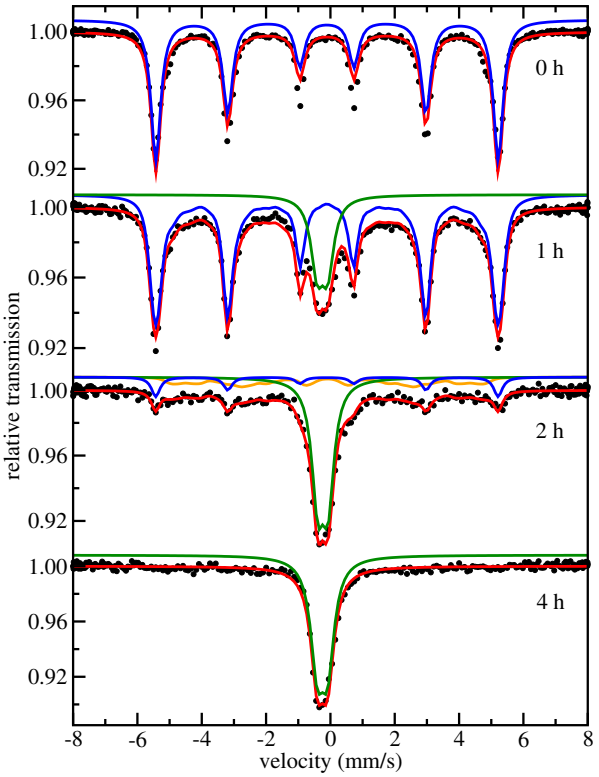

Fig. 2 Mössbauer spectra of samples milled at 400 rpm

increase in the lattice parameter of the bcc Fe phase and a slight decrease in the lattice parameter of the bcc Mo phase as a function of milling time. Considering that the atomic radius of molybdenum is larger than that of iron, this result suggests the incorporation of Fe into the Mo matrix and Mo in the Fe matrix. In other words, X-ray diffraction indicates the formation of two phases: a bcc Fe–Mo solid solution with a lattice parameter close to that of metallic Fe and a bcc Mo–Fe solid solution with a lattice parameter close to that of metallic Mo. These phases will be identified as bcc Fe and bcc Mo, as shown in Table 1.

Table 1 also shows average particle sizes, *d*, obtained using the Scherrer equation. It is important to point out that the Scherrer equation does not separate the effects of particle size and residual microstrain; therefore, the values of particle size presented in the table tend to be consistently underestimated. Regardless of that, an expected reduction in particle size is observed as a result of milling. It can also be observed that, despite the diffusion of atoms from one matrix to the other, the average particle size of both bcc Fe and bcc Mo phases follows a similar process of size reduction, remaining in the same order of magnitude with the particles of the bcc Fe phase consistently smaller.

The X-ray diffraction results show that milling induces Fe diffusion in the Mo matrix and vice versa. This can also be

Table 1 Lattice parameters *a* (in Å) and average particle size *d* (in nm) of bcc-Fe and bcc-Mo phases milled at 400 and 500 rpm

Milling time (h)	bcc-Fe		bcc-Mo	
	a	*d*	*a*	*d*
400 rpm				
0	2.865		3.146	
1	2.866	12	3.143	15
2	2.899	6	3.141	8
4	2.904	6	3.137	8
500 rpm				
0.5	2.866	16	3.144	20
1	2.874	6	3.142	10
2	2.914	5	3.141	8
3	2.921	5	3.139	7

observed in the Mössbauer spectra by the analysis of their spectral components. Metallic iron is ferromagnetic and its Mössbauer spectrum is a sextet with well-defined hyperfine parameters ($B_{hf} = 33\,T$, $\delta = 0\,mm/s$ and $\Delta = 0\,mm/s$). As metallic molybdenum does not have a magnetic moment, its presence in the vicinity of a Fe atom tends to reduce the hyperfine magnetic field on Fe nuclei, changing the Mössbauer spectrum [4]. This reduction of the hyperfine magnetic field is proportional to the number of Mo atoms in the

vicinity of a Fe atom. In the limit, the hyperfine field goes to zero and the Mössbauer spectrum changes from a sextet to a doublet or a singlet.

The Mössbauer spectra of the samples are shown in Fig. 2. Experimental data are shown as black circles while fits are shown as color lines. The spectrum of the unmilled sample (0 h) was fitted with only one sextet (blue line) with hyperfine parameters corresponding to α-Fe. The spectrum of the sample with 1 h of milling time shows the presence of a paramagnetic doublet (green line) in addition to the α -Fe sextet. This doublet may be associated with iron atoms with a majority of Mo neighbors, either in the bcc Fe or bcc Mo phases [3]. During the course of milling, the doublet relative area increases relative to that of the sextet, as can be observed in the spectrum of the sample milled for 2 h. A third spectral component in the form of a magnetic field distribution (orange line) can also be observed. This distribution is also associated with the bcc Fe and/or bcc Mo phases and corresponds to Fe sites with various configurations of Mo neighbors that are not enough to bring the hyperfine field on the Fe nuclei to zero. At the end of the milling process, the entire sextet is converted into a doublet, as can be seen in the spectrum of the sample with 4 h of milling.

It is important to note that X-ray diffraction does not allow the identification of a crystallographic phase clearly being transformed, which makes it difficult to study the kinetics of the reaction. By Mössbauer spectroscopy, on the other hand, it is possible to identify two magnetic phases that undergo transformation during the course of milling: a ferromagnetic phase of α-Fe (sextet) and a paramagnetic phase of Fe (doublet) with majority neighbors of Mo atoms. During milling, the former phase is transformed into the latter, passing through an intermediate phase corresponding to the hyperfine field distribution. Either phase can be used to study the reaction kinetics.

A second set of samples was produced with an angular velocity of 500 rpm. The same procedure was carried out and results similar to those from the 400 rpm experiment were obtained, as can be seen in Figs. 3 and 4 and Table 1. Solid solutions of Fe–Mo (bcc Fe) and Mo–Fe (bcc Mo) were obtained with the observation of a clear phase transformation from ferromagnetic α-Fe to paramagnetic Fe with a majority of Mo atoms as neighbors. The higher velocity of 500 rpm influenced the reaction kinetics by making them faster as the phase transformation is completed after only 3 h of milling, as opposed to the 4 h observed from the 400 rpm results. We have not investigated the existence of other possible phase transformations after longer milling times.

3.1 Reaction kinetics

As observed in the previous section, X-ray diffraction allows the identification of two crystallographic phases, namely

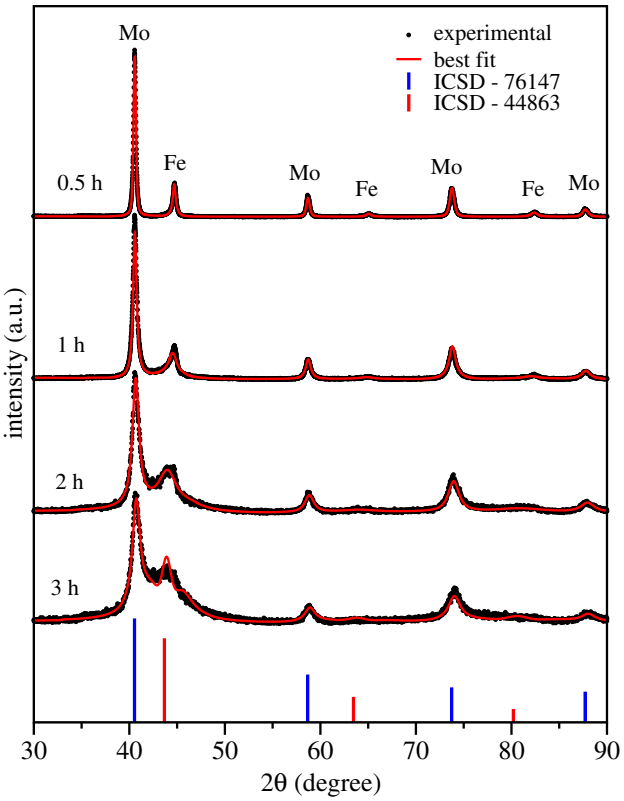

Fig. 3 X-ray patterns of samples milled at 500 rpm

bcc Fe and bcc Mo. These phases correspond to solid solutions of Fe–Mo in the bcc matrix of Fe and Mo–Fe in the bcc matrix of Mo, respectively. Neither of these two phases undergo a clear transformation that can be accompanied by the evolution of their volume. Using Mössbauer spectroscopy, it is possible to identify two magnetic phases: a ferromagnetic α-Fe phase represented by a sextet and a paramagnetic phase of Fe with a majority of Mo neighbors, represented by a doublet. The reaction kinetics of the transformation (sextet being transformed into a doublet passing through an intermediate phase corresponding to the hyperfine field distribution) may be accompanied by the evolution of their volumes, which can be obtained by the relative areas of the respective subspectra in Figs. 2 and 4.

Phase decomposition and formation induced by solid-state reactions are often empirically described by JMA-type equations. The JMA expression for phase decomposition is given by

$$V(t) = V_0 \, e^{-(kt)^n}, \tag{2}$$

where $V(t)$ is the unreacted volume at time t, V_0 is the initial volume, k is a reaction rate, usually described by an Arrhenius equation in terms of the temperature and activation energy, and n is the Avrami exponent, which depends on the growth mechanism and dimensionality [25, 31]. The values

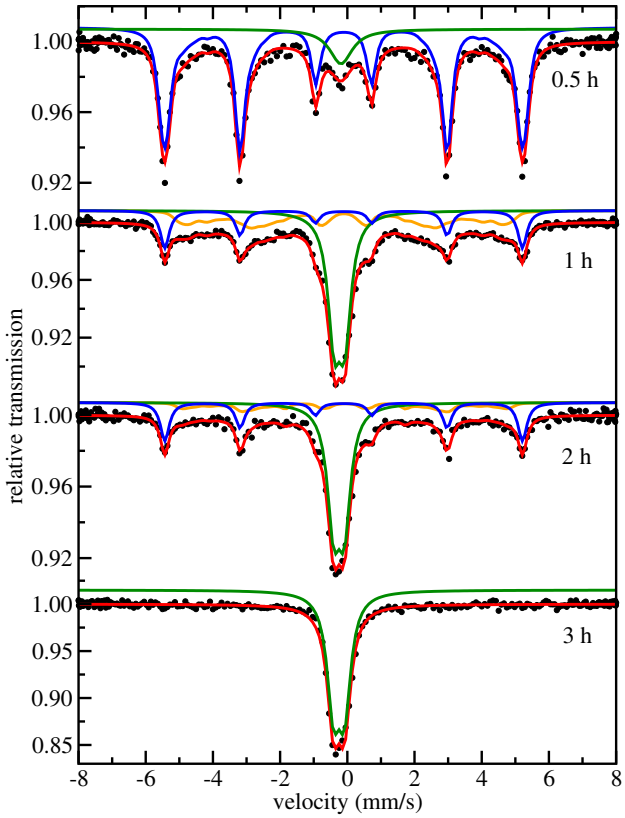

Fig. 4 Mössbauer spectra of samples milled at 500 rpm

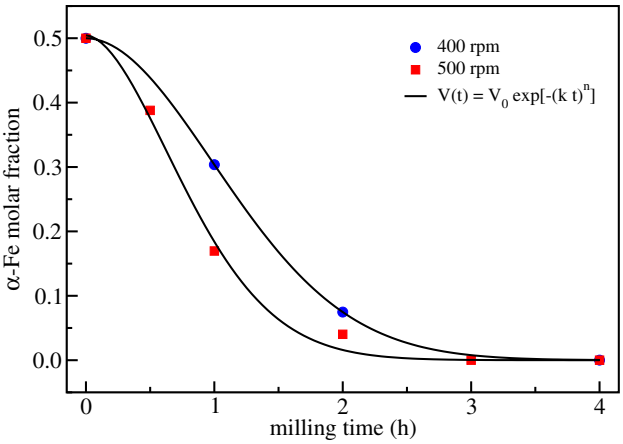

Fig. 5 Time evolution of α-Fe molar fraction in the samples of Fe–Mo milled at 400 and 500 rpm. Solid lines are fits to the data using Eq. 2

of k and n provide an indication to what type of mechanisms are dominant during the reaction and how fast these mechanisms work [25, 32].

The kinetics law of Eq. (2) was successfully applied to study solid-state reactions, like the formation/decomposition of Fe–Mo [7, 8], Fe–Cr–Mo [9], Fe–Co–Ni [11], Fe–Co [12], Fe–Cu and Fe–N [18], Fe–Mo–C [21], Cu [25], a $AlH_3/MgCl_2$ nanocomposite [26], Fe–Cr [33] and $NaNH_2$-MgH_2 powder mixtures [34]. Many more examples can be found in the literature.

Therefore, it is reasonable to assume that Eq. (2) can be applied to model the time evolution of either the ferromagnetic or the paramagnetic phase volume. We chose to study the reaction kinetics of the ferromagnetic phase. As the alloy has a Fe concentration of 50 at.%, it is reasonable to suggest that the areas of the subspectra shown in Figs. 2 and 4 represent 50 at.% of the sample volume. Following this reasoning, the spectral areas of the Mössbauer sextets were used to calculate the time evolution of the molar fraction of α-Fe in the total volume of material shown in Fig. 5. The circles and squares in the figure represent the experimental values obtained from the sextet areas in the Mössbauer spectra. The solid lines represent the best fit of Eq. (2) to the experimental data. The uncertainties are those obtained by the fitting procedure and are typically lower than 2%. The molar fraction of α-Fe at $t = 0$ is 0.5 in both curves because all the iron atoms are in this phase. The milling process induces the formation of solid solutions resulting in the appearance of the paramagnetic phase at the expense of α-Fe, whose volume suffers a gradual decrease with milling time. The reaction is completed when the whole α-Fe is transformed and its volume is zero. These results confirm the initial assumption that the JMA model applies to the system under study.

The tribochemical activity to destroy the α-Fe phase can be written based on Eq. (1) as

$$\xi^{\alpha\text{-Fe}}(t) \propto \frac{\mathrm{d}V_{\alpha\text{-Fe}}(t)}{\mathrm{d}t} \frac{1}{V_{\alpha\text{-Fe}}(t)\left[1 - V_{\alpha\text{-Fe}}(t)\right]}, \tag{3}$$

where $V_{\alpha\text{-Fe}}(t)$ is the volume of α-Fe at a given time t obtained by the fits to the curves in Fig. 5. Figure 6 shows the tribochemical activity versus milling time for the samples milled at 400 and 500 rpm. They show high reactivity at the beginning of the process ($\mathrm{d}\xi/\mathrm{d}t$ is large for $t = 0$), which indicates that the reactivity is proportional to the concentration gradient between α-Fe and the Mo-rich phase. The reaction rate increases due to the increase of interfaces between the two phases (grain size reduction and element diffusion). It can also be seen that the absolute value of $\xi^{\alpha\text{-Fe}}$ is a monotonic function of time showing that saturation is not reached and that the reactive capacity of the reactants does not decrease, i.e., the reaction stops due to the lack of reactants.

The $\xi^{\alpha\text{-Fe}}$ values at 500 rpm are consistently larger (in modulus) than those at 400 rpm. Increasing the milling rotation speed leads to both increased kinetic energy (larger impact energies) and an increased number of impacts (higher impact frequency). The effect of rotation speed in the reaction kinetics can be evaluated by substituting Eq. (2) into Eq. (3) to obtain

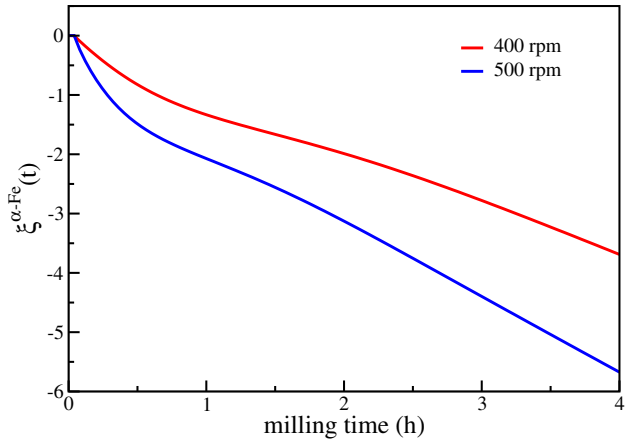

Fig. 6 Tribochemical activity to destroy α-Fe for Fe–Mo samples milled at 400 and 500 rpm

Table 2 Coefficients obtained by fitting Fig. 6 to Eq. 4

	V_0	$k\,(\mathrm{h}^{-1})$	n
400 rpm	0.49	0.70	1.9
500 rpm	0.50	1.00	1.8

$$\xi^{\alpha\text{-Fe}}(t) \propto -\frac{nk^n t^{n-1}}{1 - V_0\, \mathrm{e}^{-(kt)^n}}. \tag{4}$$

Equation (4) is then used to fit the tribochemical affinities of Fig. 6. The coefficients resulting from the fits are listed in Table 2.

The values of n from both experiments are very similar suggesting the same mechanism is responsible for phase transformation regardless of rotation speed. Theoretically, n ranges from 1.5 to 2.5 for zero or decreasing nucleation rate, whereas it is larger than 2.5 for constant or increasing nucleation rate. The value of n was also found to be correlated with the impact energies [35].

The values of k, on the other hand, are markedly different with a large reaction rate at 500 rpm. As the main role of impact frequency is to increase the speed of the reaction [23], these values of k and n suggest that impact frequency, and not impact energy, is the effect of changing rotational speeds that affects significantly the reaction kinetics of the Fe–Mo system of this study. The behavior of the tribochemical activity of this Fe–Mo system is similar to that observed for a Fe–N system previously published [18]. The Fe–Mo and Fe–N systems have in common the fact that both are formed by exothermic reactions (with a negative enthalpy of mixture). The behavior of ξ for an endothermic system (with positive enthalpy of mixing), such as Fe–Cu, is markedly different [18]. The presence of a stationary stage (with $\xi = 0$) at the end of the Fe–Cu endothermic reaction suggests that saturation is reached and there may be unreacted material left in the sample, which does not occur in the exothermic reactions of Fe–Mo and Fe–N, where saturation is not achieved.

4 Conclusions

Equiatomic Fe–Mo solid solutions produced by mechanical alloying were characterized by X-ray diffraction and Mössbauer spectroscopy. It was possible to clearly identify a phase transformation from ferromagnetic α-Fe (sextet) to paramagnetic Fe with a majority of neighboring Mo atoms (doublet) passing through an intermediate phase (hyperfine field distribution), as a result of milling. The time evolution of the ferromagnetic phase volume was fitted using the JMA equation showing its wide scope of applications. The transformation kinetics of the ferromagnetic phase were studied using a model based on the phase volume transformations represented by the tribochemical activity.

The time evolution of the tribochemical activity presented similar behavior for reactions performed at 400 and 500 rpm, with the values at 500 rpm consistently larger (in modulus). The values of JMA coefficients suggest that impact frequency, and not impact energy, is the dominant effect on the reaction kinetics due to changing milling rotational speeds in the range studied.

The tribochemical activity showed a high reactivity at the start of the process, followed by an increase (in magnitude) of the reaction rate, indicating that the reactivity is related to the concentration gradient and the contact surfaces between the phases. The absolute value of tribochemical activity is a monotonic function of time of time showing that saturation is not reached and that the reactive capacity of the reactants does not decrease.

It was observed that the behavior of the tribochemical activity for Fe–Mo is similar to that for Fe–N, published elsewhere, which can be explained by the fact that these are both exothermic reactions (with a negative enthalpy mixture). The behavior of the tribochemical activity for the endothermic system (with a positive enthalpy) Fe–Cu, also published elsewhere, is markedly different.

Acknowledgements The authors are grateful to the Brazilian research agencies Fundação Cearense de Apoio ao Desenvolvimento Científico e Tecnológico (FUNCAP), Conselho Nacional de Desenvolvimento Científico e Tecnológico (CNPq) for financial support.

References

1. Y. Jiraskova, K. Zabransky, I. Turek, J. Bursik, D. Jancik, Microstructure and physical properties of mechanically alloyed Fe–Mo powder. J. Alloy Compd. **477**, 55 (2009)

2. V.V. Kuznetsov, K.E. Golyanin, T.V. Pshenichkina, B.F. Lyakhov, S.E. Lyashenko, Chemical composition of Fe–Mo alloys obtained by electrodeposition. Mendeleev Commun. **23**, 331 (2013)
3. J. Cieślak, S.M. Dubiel, M. Reissner, Magnetism of α-phase FeMo alloys: Its characterization by magnetometry and Mössbauer spectrometry. J. Magn. Magn. Mater. **401**, 751 (2016)
4. J. Przewoźnik, S.M. Dubiel, Magnetism of α-phase Fe–Mo alloys: ac magnetic susceptibility study. J. Alloys Compd. **630**, 222 (2015)
5. R. Idczak, R. Konieczny, J. Chojcan, Study of defects in Fe–Re and Fe–Mo alloys by the Mössbauer and positron annihilation spectroscopies. Solid State Commun. **152**, 1924 (2012)
6. R. Idczak, R. Konieczny, J. Chojcan, Short-range order in iron alloys studied by ^{57} Fe Mössbauer spectroscopy. Solid State Commun. **159**, 22 (2013)
7. H. Moumeni, S. Alleg, J. Greneche, Formation of ball-milled FeMo nanostructured powders. J. Alloys Compd. **419**, 140 (2006)
8. H. Moumeni, A. Nemamcha, S. Alleg, J.M. Grenèche, Hyperfine interactions and structural features of Fe–44Co–6Mo (wt.%) nanostructured powders. Mater. Chem. Phys. **138**, 209 (2013)
9. J. Park, G. Jeong, S. Kang, S.-J. Lee, H. Choi, Fabrication of Fe–Cr–Mo powder metallurgy steel via a mechanical-alloying process. Met. Mater. Int. **21**, 1031 (2015)
10. M.A. Eryomina, S.F. Lomayeva, A.L. Ul'yanov, E.P. Yelsukov, Structural and phase transformations during copper and iron mechanical alloying in liquid medium studied by Mössbauer spectroscopy. Met. Mater. Int. **22**, 163 (2016)
11. P. Loginov, D. Sidorenko, E. Levashov, Mechanical alloying as an effective way to achieve superior properties of Fe–Co–Ni binder alloy. Metals **7**, 570 (2017)
12. R. Konieczny, R. Idczak, Thermodynamic properties of dilute Co–Fe solid solutions studied by ^{57} Fe Mössbauer spectroscopy. Nukleonika **62**, 109 (2017)
13. T. Pikula, Local atomic arrangement in mechanosynthesized $Co_x Fe_{1-x} Ni_y$ alloys studied by Mössbauer spectroscopy. Appl. Phys. A **117**, 1491 (2014)
14. T.P. Braga, D.F. Dias, M.F. Sousa, J.M. Soares, J.M. Sasaki, Synthesis of air stable FeCo alloy nanocrystallite by proteic sol-gel method using a rotary oven. J. Alloy Compd. **622**, 408 (2015)
15. C.M. Santos, A.F.N. Martins, B.C. Costa, T.S. Ribeiro, T.P. Braga, J.M. Soares, J.M. Sasaki, Synthesis of FeNi alloy nanomaterials by proteic solgel method: Crystallographic, morphological, and magnetic properties. J. Nanomater. **2016**, 1 (2016)
16. R. Idczak, K. Idczak, R. Konieczny, Oxidation and surface segregation of chromium in Fe-Cr alloys studied by Mössbauer and X-ray photoelectron spectroscopy. J. Nucl. Mater. **452**, 141 (2014)
17. C. Suryanarayana, Mechanical alloying and milling. Prog. Mater Sci. **46**, 1 (2001)
18. I.F. Vasconcelos, R.S. de Figueiredo, Transformation kinetics on mechanical alloying. J. Phys. Chem. B **107**, 3761 (2003)
19. S. Torkan, A. Ataie, H. Abdizadeh, S. Sheibani, Effect of milling energy on preparation of nano-structured $Fe_{70} Si_{30}$ alloys. Powder Technol. **267**, 145 (2014)
20. P. Baláz, M. Achimovicová, M. Baláz, P. Billik, Z. Cherkezova-Zheleva, J.M. Criado, F. Delogu, E. Dutková, E. Gaffet, F.J. Gotor, R. Kumar, I. Mitov, T. Rojac, M. Senna, A. Streletskii, K. Wieczorek-Ciurowa, Hallmarks of mechanochemistry: From nanoparticles to technology. Chem. Soc. Rev. **42**, 7571 (2013)
21. L. Kong, Y. Liu, J. Liu, Y. Song, S. Li, Y. Liang, Y. Zheng, W. Cui, Kinetics of the austenitization in the Fe–Mo–C ternary alloys during continuous heating. Open Phys. **14**, 695 (2016)
22. T. Kirindi, U. Sari, M. Kurt, Mössbauer and electron microscopy study of martensitic transformations in an Fe–Mn–Mo alloy. Int. J. Miner. Metall. Mater. **17**, 448 (2010)
23. I.F. Vasconcelos, R.S. de Figueiredo, Driving mechanisms on mechanical alloying: Experimental and molecular dynamics discussions. Nanostruct. Mater. **11**, 935 (1999)
24. J. Cieślak, B.F.O. Costa, S.M. Dubiel, G.L. Caër, Kinetics of the sigma-to-alpha phase transformation caused by ball milling in near equiatomic Fe–Cr alloys. Phys. Rev. B **73**, 184123 (2006)
25. S. Sheibani, A. Ataie, S. Heshmati-Manesh, Kinetics analysis of mechano-chemically and thermally synthesized Cu by Johnson–Mehl–Avrami model. J. Alloys Compd. **455**, 447 (2008)
26. C.W. Duan, L.X. Hu, Y. Sun, H.P. Zhou, H. Yu, Reaction kinetics for the solid state synthesis of the AlH_3/ $MgCl_2$ na no-composite by mechanical milling. Phys. Chem. Chem. Phys. **17**, 22152 (2015)
27. I. Lucks, P. Lamparter, E.J. Mittemeijer, Uptake of iron, oxygen and nitrogen in molybdenum during ball milling. Acta Mater. **49**, 23578 (2001)
28. H.M. Rietveld, Line profiles of neutron powder-diffraction peaks for structure refinement. Acta Cryst. **22**, 151 (1967)
29. H.M. Rietveld, A profile refinement method for nuclear and magnetic structures. J. Appl. Cryst. **2**, 65 (1969)
30. L. Bleicher, J.M. Sasaki, C.O. Paiva-Santos, Development of a graphical interface for the Rietveld refinement program DBWS. J. Appl. Crystallogr. **33**, 1189 (2000)
31. M.A. Bab, L. Mendoza-Zélis, L.C. Damonte, Nanocrystalline HfN produced by mechanical milling: Kinetic aspects. Acta Mater. **49**, 4205 (2001)
32. Y. Shen, H.H. Hng, J.T. Oh, Formation kinetics of Ni-15%Fe-5% Mo during ball milling. Mater. Lett. **58**, 2824–2828 (2004)
33. R. Idczak, Internal oxidation process in diluted Fe–Cr alloys: A transmission Mössbauer spectroscopy study. Appl. Phys. A **122**, 1009 (2016)
34. S. Garroni, F. Delogu, C.B. Minella, C. Pistidda, S. Cuesta-Lopez, Mechanically activated metathesis reaction in $NaNH_2$-MgH_2 powder mixtures. J. Mater. Sci. **52**, 11891 (2017)
35. F. Miani, P. Matteazzi, D. Basset, Mechanosynthesis of iron carbides at composition Fe75C25: Modeling of the process kinetics. J. Alloys Compd. **204**, 151 (1994)